Comparing One- and Two-Dimensional Heteronanostructures As Silicon-Based Lithium Ion Battery Anode Materials

Jin Xie,[†] Xiaogang Yang,[†] Sa Zhou, and Dunwei Wang*

Department of Chemistry, Merkert Chemistry Center, Boston College, 2609 Beacon Street, Chestnut Hill, Massachusetts 02467, United States. [†]These authors contributed equally.

ABSTRACT The performance of advanced energy conversion and storage devices, such as solar cells, supercapacitors, and lithium (Li) ion batteries, is intimately connected to the electrode design at the nanoscale. To enable significant developments in these research fields, we need detailed information about how the properties of the electrode materials depend on their dimensions and morphologies. This information is currently unavailable, as previous studies have mostly focused on understanding one type of morphology at a time. Here, we report a systematic study to compare the performance of nanostructures enabled by two platforms, one-dimensional nanowires and two-dimensional nanonets. The nanowires and nanonets shared the same composition (titanium disilicide) and similar sizes. Within the framework of Li ion battery applications, they exhibited different stabilities upon lithiation and delithiation (at a rate of 6 A/g), the nanonets-based nanostructures maintaining 90% and the nanowires-based ones 80% of their initial stable capacities after 100 cycles of repeated charge and discharge. The superior stability of the nanonets was ascribed to the two-dimensional connectivity, which afforded better structural stability than nanowires. Information generated by this study should contribute to the design of electrode materials and thereby enable broader applications of complex nanostructures for energy conversion and storage.

KEYWORDS: lithium ion batteries · nanostructures · nanonets · nanowires · silicide

Being able to design, synthesize, and understand electrode materials with desired chemical, electronic, ionic, and physical properties plays a critical role in the development of advanced energy conversion and storage technologies, such as solar cells, rechargeable batteries, and supercapacitors. We consider the Li ion battery as an example. Despite its many advantages over other competing energy storage technologies, there is plenty of room for improvements in terms of power rate, cycle lifetime, and safety.[1−5] Among various considerations, that concerning power rate is worth particular research attention because solutions to this problem will involve the creation of materials with *both* high ionic and high electronic conductivity, a fundamental challenge in materials science.[6] Achieving high power rate is also of great practical implications, as it will greatly broaden where and how Li ion batteries can be used. Indeed, a great deal of research has been attracted to solving this challenge, including efforts to discover new compounds, new crystal structures, or both.[1,7] Because the properties of materials are intimately connected to the designs at the nanoscale, considerable attention has been paid to using nanostructures as Li ion battery electrodes.[4,8] For instance, nanoparticles,[9] nanowires,[10] and three-dimensional (3D) complex nanostructures[5] have been widely reported to exhibit new and improved performance on this front.

More recently, approaches to using multiple nanoscale components to form heteronanostructures have been proposed and reported by others and us.[11−18] In a heteronanostructure, nanowires,[13] nanotubes,[14] nanonets,[17] graphene,[18] or 3D nanostructures[19] serve as structural support and charge transporter. On them are active material coatings, in the form of thin films or nanoparticles. With the fine features of the active materials at the nanoscale, the total time required for ionic diffusion is short; with the overall morphology at the micrometer scale, electronic charge transport is fast. As such this strategy allows for the measurement of combined large capacity, high power rate, and long cycle lifetime that cannot be measured on single-component materials and therefore has great potential to dramatically advance Li ion battery research. To materialize these potentials, we need a detailed understanding of how the performance of the resulting heteronanostructures depends on the fine features. This

* Address correspondence to dunwei.wang@bc.edu.

Received for review September 9, 2011 and accepted October 13, 2011.

Published online October 13, 2011
10.1021/nn203480h

requires systematic studies to compare the properties of heteronanostructures of similar compositions and comparable sizes but different morphologies. Due to the diversity of materials studied, however, little has been done to this end. In this article, we take the initiative to compare Si-based anode materials that involve two-dimensional (2D) and one-dimensional (1D) $TiSi_2$ nanostructures and show that the morphology indeed influences the properties of the heteronanostructures to a measurable extent.

Our study is enabled by the unique $TiSi_2$ system, where we can produce either 2D nanonets or 1D nanowires of the same composition and similar sizes by adjusting the synthesis chemistry.[20−23] They both can be interfaced with Si to act as structural supports, which will solve the poor stability issue, and charge transporters, which will meet the low conductivity challenge of Si. Although of similar sizes to 1D nanowires, the fine structures of the 2D nanonets are interconnected, providing a suitable platform to study how the complexity of the morphology influences the electrode materials' properties. Our results show that when the $TiSi_2$ is protected from reactions with Li^+, the nanonets exhibit better stability than the nanowires do. The difference is attributed to the multiconnectivity of the nanonets, which reduces failures due to the mechanical breakdown of individual $TiSi_2$ beams.

RESULTS AND DISCUSSION

Design Considerations. The basis for our study is illustrated schematically in Figure 1. The design has two parts: $TiSi_2$ nanowires or nanonets and Si nanoparticles. Our previous study reveals that having Si in the particulate form (Figure 1a, c) is advantageous because the space between adjacent particles allows for volume expansion and reduction during lithiation (charge) and delithiation (discharge) of Si, respectively, thereby minimizing stress buildup during the processes.[17] Under idealized operating conditions, the $TiSi_2$ support remains intact during repeated charge and discharge processes, and the eventual degradation of Si would be the main failing mechanism. In practice, however, a number of processes can cause failures of the $TiSi_2$ nanowires and nanonets, consequently the failures of the electrode materials. The present study concerns one of these failing mechanisms, the mechanical breakdown of the nanowires and nanonets (Figure 1b, d). Factors that can contribute to this mechanism include lithiation-induced stress on the surfaces, unwanted chemical reactions of $TiSi_2$ with the electrolyte, and overheating, among others. The advantage of the nanonets-based design is obvious when such breakdown happens. In the case of nanowires, due to the loss of electrical contact with the current collector, the portion of the heteronanostructure beyond the cracking point will become inaccessible, as shown in Figure 1b, reducing the overall

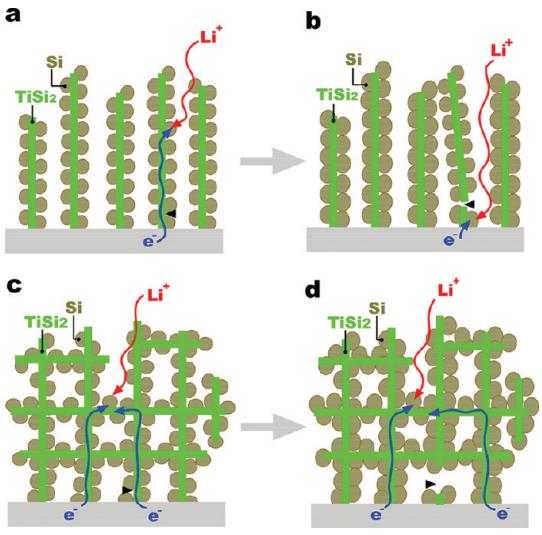

Figure 1. Schematic comparison of the nanowires- and nanonets-based systems. The basis for the designs is identical, i.e., to form Si nanoparticles on the nanowires (a) or the nanonets (c). In both cases, the nanowires or the nanonets serve as structural supports and charge transporters. The ionic and electronic pathways are illustrated by red and blue arrows, respectively. The difference is manifested when a mechanical breakdown occurs. (b) The portions of the nanowire beyond the breaking point will be inaccessible because of the loss of electrical contact. (d) Owing to the existence of other charge transport pathways within the nanonets, the breakdown of a single beam will have limited impact on the overall capacity.

capacity. In the case of nanonets, such breakdown will have relatively limited influence on the overall capacity since the portions beyond the breaking point can still be connected to the current collector through other routes, as shown in Figure 1d. The overall capacity will fade at a comparatively slower pace than that of the nanowires-based nanostructures.

Structural Characterizations. The synthesis of $TiSi_2$ nanonets/Si heteronanostructures has been reported previously by us.[17] That of $TiSi_2$ nanowires/Si nanostructures is a new development, as our previous study concerned only the $TiSi_2$ nanowires without intentional Si deposition.[22] The parameters to deposit Si nanoparticles onto nanowires and nanonets were the same as detailed in the Experimental Section. The resulting nanostructures were characterized by a scanning electron microscope (SEM) and a transmission electron microscope (TEM). As can be seen in Figure 2, the fine features of the nanowires (Figure 2a, b) and the nanonets (Figure 2c, d) were of comparable sizes (diameters ~15−20 nm; lengths ~1−5 μm). The as-deposited Si nanoparticles were uniform and approximately 20−30 nm in diameter. Elemental analysis by energy dispersive spectroscopy (EDS) showed that the overall Si content (including that from $TiSi_2$) accounted for ca. 90% (wt %).

Comparison of Stabilities upon Repeated Charge/Discharge. To study the stabilities of $TiSi_2$ nanonets/Si and $TiSi_2$ nanowires/Si nanostructures, we assembled coin cells with the as-made materials as anodes. Li foils were

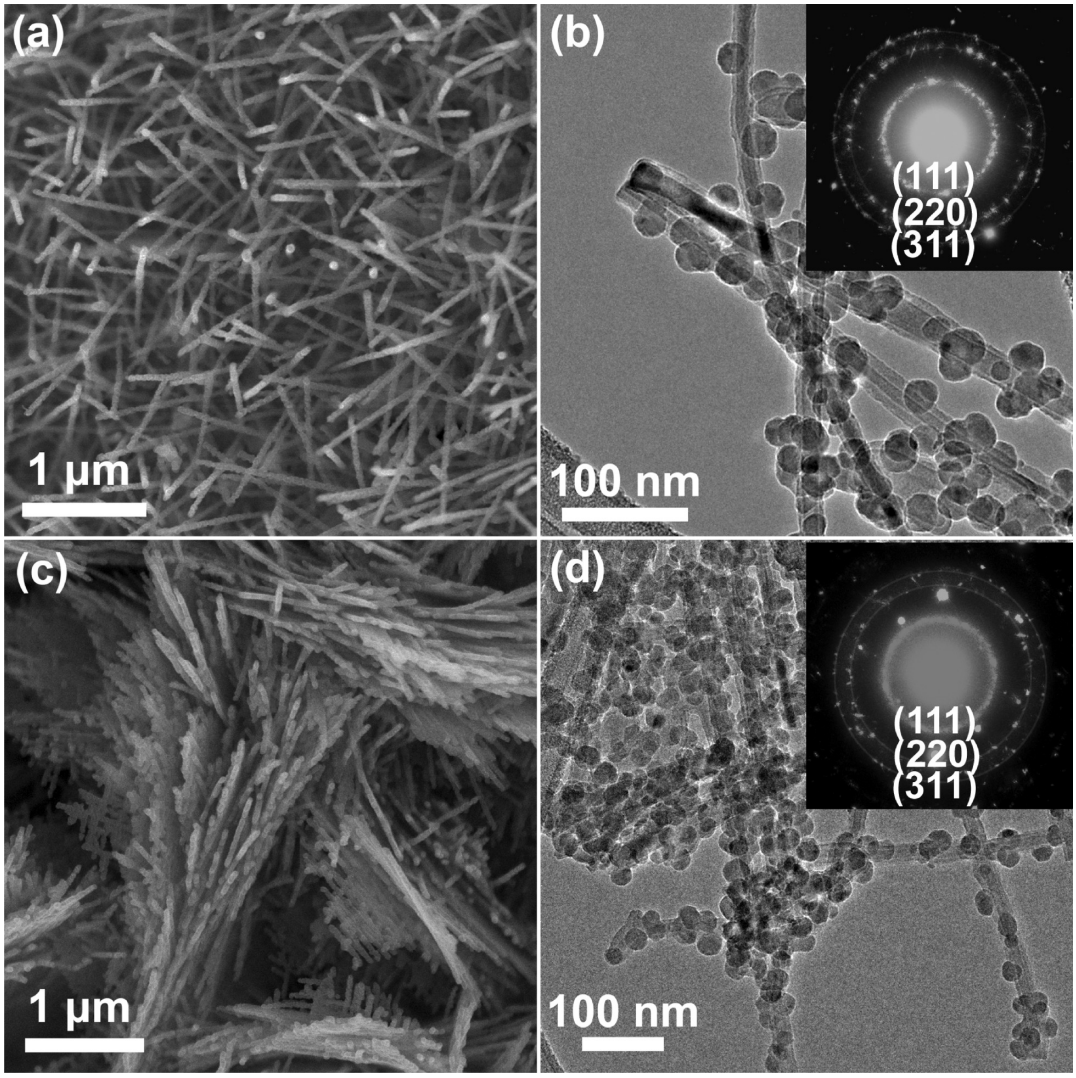

Figure 2. Structural characterizations of $TiSi_2$ nanowires- and nanonets-based heteronanostructures. (a and b) SEM and TEM micrographs of the nanowires-based nanostructures. (c and d) SEM and TEM micrographs of the nanonets-based nanostructures. Insets in (b) and (d) are selected area electron diffraction patterns, where the diffraction spots due to crystalline Si are characteristic of polycrystalline materials (highlighted by gray rings) because the data were collected on multiple Si particles.

chosen as the cathode electrode for the ease in accurately measuring the anode potentials relative to the Li/Li^+ standard. These coin cells were then connected to a battery analyzer (more details in the Experimental Section), which passed a constant current through the cells and recorded the anode potentials as a function of time. The specific capacity was calculated by normalizing the number of charges (in units of mAh) against the total mass of the anode (in units of g). The mass of both $TiSi_2$ and Si was taken into account for the capacity calculations.

$TiSi_2$ Nanonets/Si Nanostructures. As shown in Figure 3a, the capacity increased from 2670 mAh/g to 2700 mAh/g during the first 5 cycles when tested within the potential window of 0.09−2 V (all potentials used in this article are relative to Li^+/Li unless noted). The Coulombic efficiency (CE) was 70% for the first cycle, which increased to 95.5% for the second cycle and then to 97.5% for the fifth cycle. We found it was important to carry out the first few cycles at a relatively slow rate (0.6 A/g, 0.2C, with 1C = 3000 mA/g). Otherwise, more rapid capacity fade and poorer performance than what is reported here would be measured. It has been suggested that during the first few cycles, together with other irreversible processes, the solid-electrolyte-interface (SEI) layer forms.[24] Nevertheless, we note that more research is needed to fully understand what role these initial lithiation/delithiation processes play. For the next five cycles, the operating potential window was further narrowed to within 0.15−2 V because our previous study shows that $TiSi_2$ nanonets react with Li^+ at approximately 0.09 V, and prolonged reactions at this potential will cause failures of the nanonets.[22] More on this point will be discussed later in this article. At a rate of 2.4 A/g (0.8C), the capacity changed from 1807 (6th cycle) to 1740

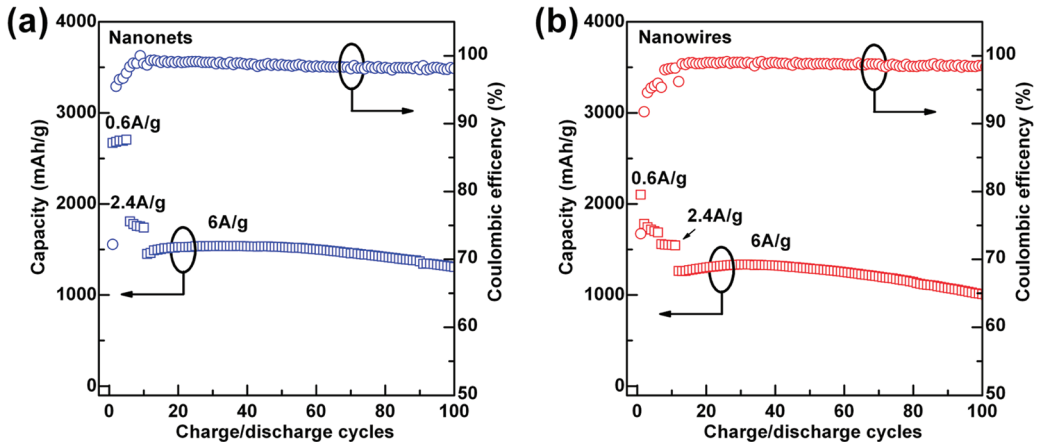

Figure 3. Cycling stability comparison of the nanonets- (a) and nanowires-based heteronanostructures (b). For clarity, only delithiation capacity is shown. The potential window for the first 5 cycles was 0.09−2 V, and that for the following tests was 0.15−2 V. The rates at which the performance was measured are labeled in the plots.

(10th cycle) mAh/g. In the meantime, the CE increased from 98.3% to 98.9%, suggesting that the lithiation/delithiation becomes more reversible after the initial charge/discharge. Afterward, the rate was changed to 6 A/g (2C). A trend of slightly increasing capacity with more charge/discharge cycles was observed until the 31st cycle, where a peak value of 1540 mAh/g was observed. Similar phenomena of capacity increase during the initial lithiation/delithiation processes have been reported before,[13] and the reason was attributed to gradually more complete lithiation of Si.[25] Significantly, 1310 mAh/g was measured after 100 cycles of test, corresponding to 90% capacity retention from the 11th cycle. The CE varied between 97.9% and 99.3%, suggesting there were still irreversible processes to contribute to the capacity loss.

$TiSi_2$ Nanowires/Si Nanostructures. Compared with the nanonets-based nanostructures, the nanowires-based one showed at least two distinct characteristics. First, despite the similarities of sizes and amount of Si loading as evidenced by the structural studies, the initial and stable capacity of the nanowire system was lower. For example, the peak specific capacity measured at 6 A/g rate was 1335 mAh/g, 13% lower than that of the nanonets-based nanostructures. At the present stage, we do not fully understand the origin of this difference but suggest that the 2D nature and the unique surface properties of the nanonets may be important factors. Second, the capacity fade from the 11th cycle to the 100th one was more obvious, from 1263 to 1008 mAh/g, ~20%.

Comparison of Stabilities under Different Operating Conditions. Our previous research has shown that $TiSi_2$ nanowires and nanonets react with Li^+ differently, the nanonets exhibiting appreciable lithiation at 0.09 V and the nanowires displaying no significant reactions down to 0.05 V.[22] With this information in mind, we next sought to examine how the operating potential windows influence the stability of the corresponding nanostructures. As can be seen in Figure 4 and similar to that in Figure 3, the nanonets-based samples showed higher capacities than the nanowire-based ones. Different from that in Figure 3, however, the capacities of the nanonets-based samples decreased more rapidly when measured at 0.05−2 V (from 2279 mAh/g at 31st cycle to 1449 mAh/g at 100th cycle) and 0.09−2 V (from 1949 mAh/g at 31st cycle to 1276 mAh/g at 100th cycle). An important reason for the more rapid capacity fade was the more complete lithiation of Si within these potential windows than that at 0.15−2 V. As such, the fading mechanism specific to Si-related reactions plays an important role here. Although secondary, the reactions between the nanonets and Li^+ at or below 0.09 V should also contribute to the relatively more rapid capacity fade for the nanonets-based materials.[22]

Structural Studies after Repeated Charge/Discharge. To understand the stability differences between the nanowires- and nanonets-based nanostructures, we examined their morphologies after 100 cycles of tests; representative SEM micrographs are shown in Figure 5. These data are to be compared with those in Figure 2. Characteristic to the Si lithiation and delithiation processes, the crystalline and particulate Si coating was transformed into amorphous, accompanied by obvious volume expansion. However, there were also nanowires whose Si coating's transformation was less profound, such as those circled by ellipses in Figure 5a, b. It is conceivable that these nanowires did not undergo the same number of lithiation and delithiation processes as their neighboring ones did probably because they were separated from the current collector after the initial reactions. Indeed, both ends of these nanowires were visible within the viewing field. Nanowires like these would not contribute to the overall capacity and thus lead to capacity fade as shown in Figures 3 and 4. From Figure 5a, we can also find a considerable number of other nanowires where

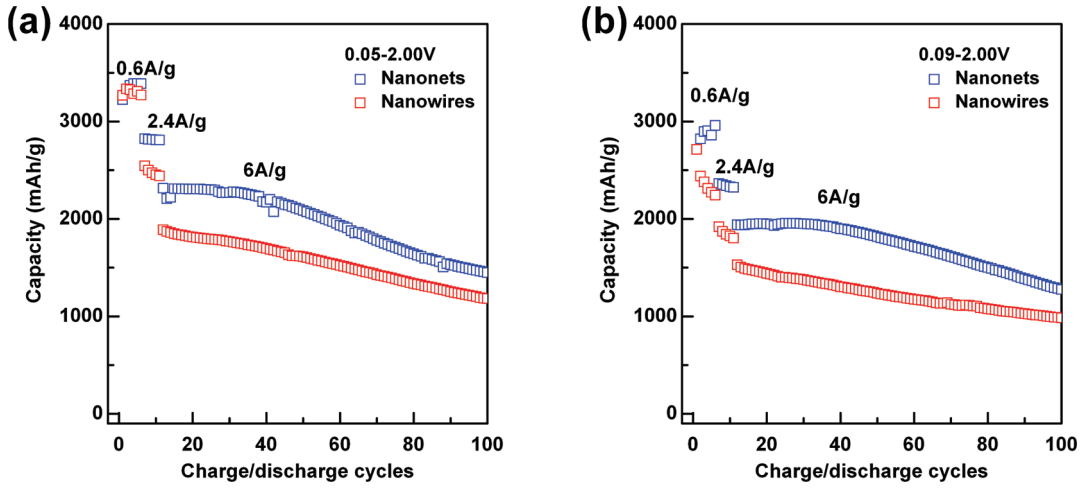

Figure 4. Stability comparison of the nanonets- and nanowires-based nanostructures. The cutoff potentials were 0.05 V (a) and 0.09 V (b). Note that the cutoff potential for data shown in Figure 3 was 0.15 V.

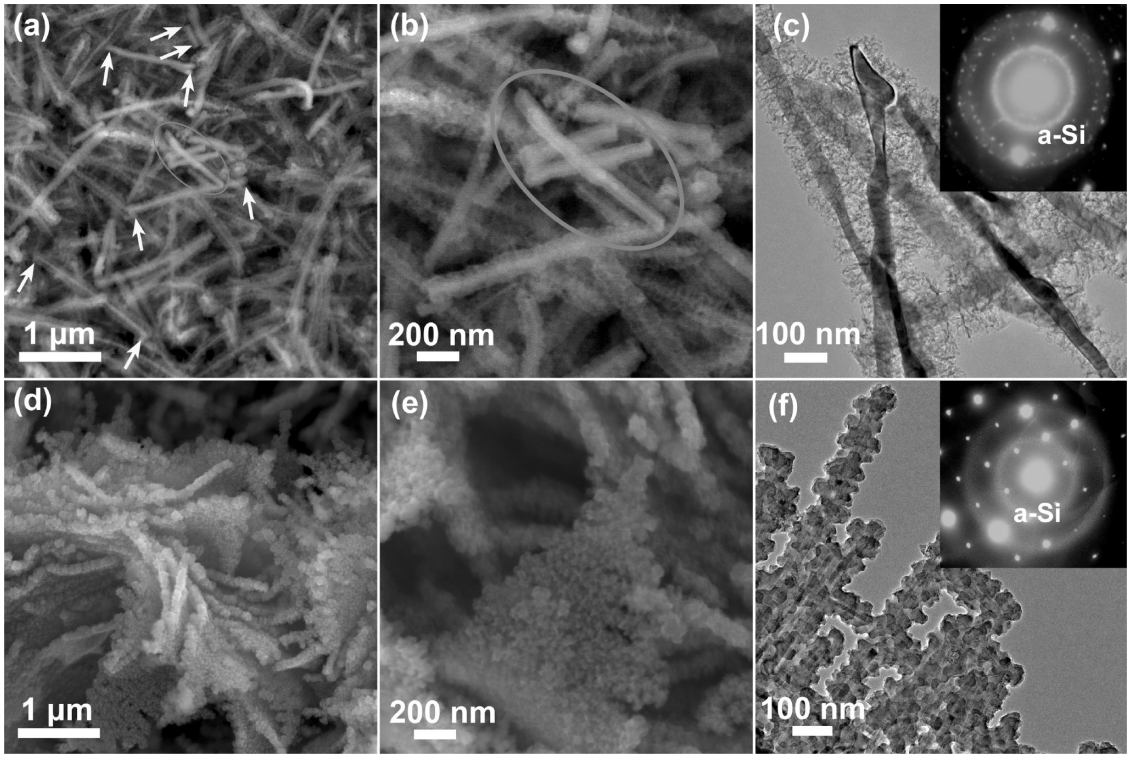

Figure 5. SEM micrographs of $TiSi_2$ nanowires- (a and b) and nanonets-based nanostructures (d and e) after 100 cycles of repeated lithiation/delithiation processes. (c and f) TEM micrographs of the same samples as in (a) and (d), respectively. The diffraction patterns (insets in c and f) indicate Si has turned amorphous during the lithiation/delithiation processes. The diffraction spots in the inset of (f) are from C49 $TiSi_2$.

both ends are visible (highlighted by arrows), indicating that they were separated from the current collector and therefore would not contribute to the overall capacity should the sample be cycled further. Few such segments were found in Figure 2a, supporting that as-grown nanowires are connected to the current collector, a feature desired for Li ion battery applications. In contrast, uniform volume expansion of Si coating was observed on nanonets-based samples, and few broken nanonets were observed, Figure 5d, e. Although more detailed studies would be needed to fully understand in which mechanism the lithiation/delithiation of Si influences the stability of the $TiSi_2$/Si systems, we emphasize that the reactions between Li^+ and the $TiSi_2$-based nanostructures are mainly limited to those with Si coatings. This point has been previously discussed by us[17,22] and is further supported by Figure 5c, f, where the $TiSi_2$ core remains unchanged after repeated charge/discharge.

Comparison of Performance at Different Charge/Discharge Rates. As discussed at the beginning of this article, one

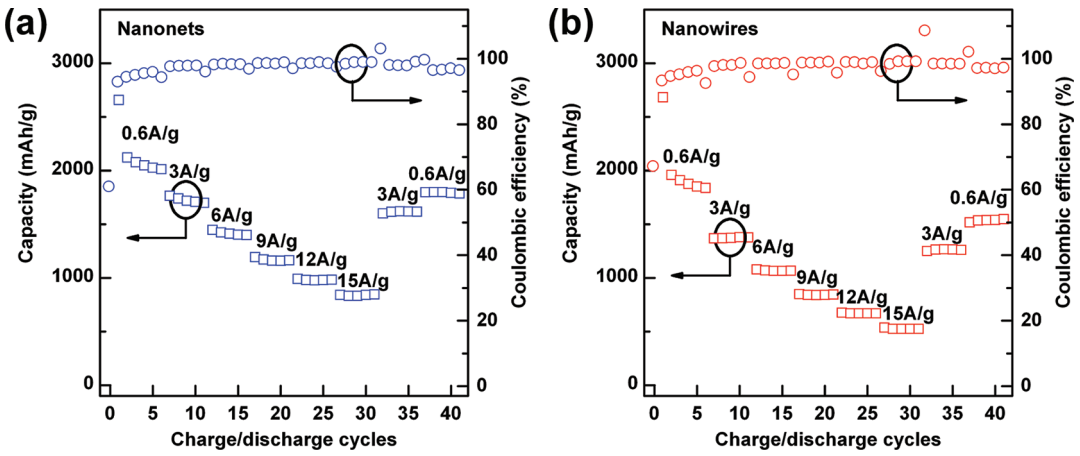

Figure 6. Comparison of nanonets- (a) and nanowires-based (b) materials at different charge/discharge rates. Because the Coulombic efficiencies were calculated by dividing the discharge capacity with the charge capacity, and these values changed dramatically when the rate was altered, we see noticeable changes of these values where the rates were varied.

key advantage of the heteronanostructure design is that it may enable high capacity *and* high power on one material at the same time. To examine this potential, we compared the nanowires- and nanonets-based nanostructures at different charge/discharge rates. As can be seen in Figure 6, the general trend was that lower capacity was measured at higher rates. For instance, a capacity of >2000 mAh/g was measured on the nanonets-based nanostructures at 0.6 A/g (0.2C); the same sample showed a capacity of ca. 800 mAh/g when measured at 15 A/g (5C). Once the rate was reduced to 3 and 0.6 A/g, the capacity increased to 1602 and 1798 mAh/g, respectively, corresponding to 75% and 85% of its original values. This trend is consistent with other literature reports of Si-based anode materials.[10,14] Slow Li^+ diffusion within Si, which results in incomplete lithiation/delithiation at high rates, is an important reason for this observation.

Although following the same general trend, the nanowires-based nanostructures exhibited noticeably poorer rate performance because the capacity dropped more quickly as the charge rate was increased, from ca. 1900 mAh/g at 0.6 A/g to ca. 530 mAh/g at 15 A/g. It increased further to 1518 mAh/g when measured again at 0.6 A/g, corresponding to 77% of its original capacity. We note the differences between nanowires- and nanonets-based materials in their performance under different rates are quasi-quantitative and as such are not sufficient for us to draw meaningful conclusions. This result nonetheless proves that the heteronanostructure design may indeed enable the measurement of high power rate because it can be charged at rates up to 15 A/g. Previously, similarly high capacities have been measured on thin films albeit at much lower rates (~2000 mAh/g on 100 nm Si thin film at C/4).[24] The loading of active materials in the heteronanostructure design can be significantly higher than that in thin films owing to the surface roughening effect. The rate performance achieved here is comparable to the reported values of 1387 mAh/g at 14 A/g for Si hollow nanosphere by Cui *et al.*[26] or 900 mAh/g at 2.5C for Si and carbon nanotube combinations by Kumta *et al.*[14]

CONCLUSIONS

In summary, we carried out a systematic study to compare how $TiSi_2$ nanowires- and nanonets-based Si nanostructures perform as anode electrode materials for Li ion batteries. Grown by similar chemistries and sharing comparable sizes, the $TiSi_2$ system offered us a unique platform to focus on how the morphology influences the properties without being confounded by factors such as composition or dimensions. Our results showed that 2D nanonets exhibited better capacity retention than 1D nanowires when measured between 0.15 and 2 V. The reason was ascribed to better structural integrity of the nanonets. We suggest that because complex nanostructures bridge length scales from angstroms to micrometers, a range highly relevant to processes fundamentally important to energy conversion and storage applications, they have great potentials as electrode materials to significantly advance research in this field.

EXPERIMENTAL SECTION

Synthesis of $TiSi_2$/Si Heteronanostructure. $TiSi_2$ nanonets were synthesized using a chemical vapor deposition method as reported by us previously.[20,23] Briefly, a Ti foil (Sigma, 0.127 mm thick, purity: 99.7%) coated with 100 nm W as the current collector was placed in a home-built reaction chamber that was heated to 675 °C, and SiH_4 (10% in He, Voltaix; 50 sccm, standard cubic centimeter per minute), $TiCl_4$ (98%, Sigma-Aldrich; 2 sccm), and H_2 (Industrial grade, Airgas; 100 sccm) flew past the surface of the Ti foil at 5 Torr. A typical growth duration was 15 min. Afterward, SiH_4 and $TiCl_4$ were stopped, and the temperature was decreased to 650 °C, after which SiH_4

(80 sccm) was introduced again for Si coating. The reaction was carried out at 15 Torr for 12 min. This process produced a particulate Si coating on the $TiSi_2$ nanowire or nanonet surfaces.

Material Characterizations. The samples before and after lithiation and delithiation processes were imaged using a transmission electron microscope (JEOL 2010F) and a scanning electron microscope (JEOL 6340F). The TEM was operated at an acceleration voltage of 200 kV, and the SEM was working at 10 kV. Elemental analysis was conducted using an energy dispersive spectroscopy attachment to the TEM.

Coin Cell Fabrication. After growth, the samples were transferred into an Ar-filled glovebox (oxygen level <1 ppm). The $TiSi_2$/Si electrodes were assembled into coin cells (CR2032-type) with Li foils as the counter electrodes, 1 M $LiPF_6$ in ethylene carbonate and diethyl carbonate (1:1, Novolyte Technologies) as the electrolyte, and two layers of polypropylene separator (25 μm, Celgard2500).

Electrochemical Measurements. The coin cells were characterized by an eight-channel battery analyzer with a battery test system (Shenzhen Neware, China) at 30 °C.

Acknowledgment. This work was supported by Boston College, NSF (DMR 1055762), and MassCEC. We thank Dr. Dezhi Wang for his help with structural characterizations.

REFERENCES AND NOTES

1. Tarascon, J. M.; Armand, M. Issues and Challenges Facing Rechargeable Lithium Batteries. *Nature* **2001**, *414*, 359–367.
2. Goodenough, J. B.; Kim, Y. Challenges for Rechargeable Li Batteries. *Chem. Mater.* **2010**, *22*, 587–603.
3. Park, M.; Zhang, X. C.; Chung, M. D.; Less, G. B.; Sastry, A. M. A Review of Conduction Phenomena in Li-Ion Batteries. *J. Power Sources* **2010**, *195*, 7904–7929.
4. Arico, A. S.; Bruce, P.; Scrosati, B.; Tarascon, J. M.; Van Schalkwijk, W. Nanostructured Materials for Advanced Energy Conversion and Storage Devices. *Nat. Mater.* **2005**, *4*, 366–377.
5. Long, J. W.; Dunn, B.; Rolison, D. R.; White, H. S. Three-Dimensional Battery Architectures. *Chem. Rev.* **2004**, *104*, 4463–4492.
6. Kang, B.; Ceder, G. Battery Materials for Ultrafast Charging and Discharging. *Nature* **2009**, *458*, 190–193.
7. Hautier, G.; Fischer, C. C.; Jain, A.; Mueller, T.; Ceder, G. Finding Nature's Missing Ternary Oxide Compounds Using Machine Learning and Density Functional Theory. *Chem. Mater.* **2010**, *22*, 3762–3767.
8. Bruce, P.; Scrosati, B.; Tarascon, J. M. Nanomaterials for Rechargeable Lithium Batteries. *Angew. Chem., Int. Ed.* **2008**, *47*, 2930–2946.
9. Poizot, P.; Laruelle, S.; Grugeon, S.; Dupont, L.; Tarascon, J. M. Nano-Sized Transition-Metaloxides as Negative-Electrode Materials for Lithium-Ion Batteries. *Nature* **2000**, *407*, 496–499.
10. Chan, C. K.; Peng, H.; Liu, G.; McIlwrath, K.; Zhang, X. F.; Huggins, R. A.; Cui, Y. High-Performance Lithium Battery Anodes Using Silicon Nanowires. *Nat. Nanotechnol.* **2008**, *3*, 31–35.
11. Scrosati, B.; Garche, J. Lithium Batteries: Status, Prospects and Future. *J. Power Sources* **2010**, *195*, 2419–2430.
12. Liu, R.; Duay, J.; Lee, S. B. Heterogeneous Nanostructured Electrode Materials for Electrochemical Energy Storage. *Chem. Commun.* **2011**, *47*, 1384–1404.
13. Cui, L. F.; Ruffo, R.; Chan, C. K.; Peng, H. L.; Cui, Y. Crystalline-Amorphous Core-Shell Silicon Nanowires for High Capacity and High Current Battery Electrodes. *Nano Lett.* **2009**, *9*, 491–495.
14. Wang, W.; Kumta, P. N. Nanostructured Hybrid Silicon/Carbon Nanotube Heterostructures: Reversible High-Capacity Lithium-Ion Anodes. *ACS Nano* **2010**, *4*, 2233–2241.
15. Cui, L. F.; Yang, Y.; Hsu, C.-M.; Cui, Y. Carbon-Silicon Core-Shell Nanowires as High Capacity Electrode for Lithium Ion Batteries. *Nano Lett.* **2009**, *9*, 3370–3374.
16. Wang, H. L.; Cui, L. F.; Yang, Y. A.; Casalongue, H. S.; Robinson, J. T.; Liang, Y. Y.; Cui, Y.; Dai, H. J. Mn_3O_4-Graphene Hybrid as a High-Capacity Anode Material for Lithium Ion Batteries. *J. Am. Chem. Soc.* **2010**, *132*, 13978–13980.
17. Zhou, S.; Liu, X. H.; Wang, D. W. Si/$TiSi_2$ Hetero-Nanostructures as High Capacity Anode Material for Li Ion Batteries. *Nano Lett.* **2010**, *10*, 860–863.
18. Wang, H.; Yang, Y.; Liang, Y.; Cui, L.-F.; Sanchez Casalongue, H.; Li, Y.; Hong, G.; Cui, Y.; Dai, H. $LiMn_{1-x}Fe_xPO_4$ Nanorods Grown on Graphene Sheets for Ultrahigh-Rate-Performance Lithium Ion Batteries. *Angew. Chem., Int. Ed.* **2011**, *50*, 7364–7368.
19. Rolison, D. R.; Long, J. W.; Lytle, J. C.; Fischer, A. E.; Rhodes, C. P.; McEvoy, T. M.; Bourg, M. E.; Lubers, A. M. Multifunctional 3D Nanoarchitectures for Energy Storage and Conversion. *Chem. Soc. Rev.* **2009**, *38*, 226–252.
20. Zhou, S.; Liu, X. H.; Lin, Y. J.; Wang, D. W. Spontaneous Growth of Highly Conductive Two-Dimensional $TiSi_2$ Nanonets. *Angew. Chem., Int. Ed.* **2008**, *47*, 7681–7684.
21. Zhou, S.; Liu, X. H.; Lin, Y. J.; Wang, D. W. Rational Synthesis and Structural Characterizations of Complex $TiSi_2$ Nanostructures. *Chem. Mater.* **2009**, *21*, 1023–1027.
22. Zhou, S.; Wang, D. W. Unique Lithiation and Delithiation Processes of Nanostructured Metal Silicides. *ACS Nano* **2010**, *4*, 7014–7020.
23. Zhou, S.; Xie, J.; Wang, D. W. Understanding the Growth Mechanism of Titanium Disilicide Nanonets. *ACS Nano* **2011**, *5*, 4205–4210.
24. Graetz, J.; Ahn, C. C.; Yazami, R.; Fultz, B. Highly Reversible Lithium Storage in Nanostructured Silicon. *Electrochem. Solid State Lett.* **2003**, *6*, A194–A197.
25. Koratkar, N.; Krishnan, R.; Lu, T. M. Functionally Strain-Graded Nanoscoops for High Power Li-Ion Battery Anodes. *Nano Lett.* **2011**, *11*, 377–384.
26. Yao, Y.; McDowell, M. T.; Ryu, I.; Wu, H.; Liu, N. A.; Hu, L. B.; Nix, W. D.; Cui, Y. Interconnected Silicon Hollow Nanospheres for Lithium-Ion Battery Anodes with Long Cycle Life. *Nano Lett.* **2011**, *11*, 2949–2954.